THE JOURNAL OF PHYSICAL CHEMISTRY Letters

pubs.acs.org/JPCL

Evidence for Vinylidene Production in the Photodissociation of the Allyl Radical

Chao Chen,[†] Bastiaan Braams,[†,#] David Y. Lee,[‡] Joel M. Bowman,[*,†] Paul L. Houston,[*,‡] and Domenico Stranges[§]

[†]Department of Chemistry and Cherry L. Emerson Center for Scientific Computation, Emory University, Atlanta, Georgia 30322, [‡]School of Chemistry and Biochemistry, Georgia Institute of Technology, Atlanta, Georgia 30332, and [§]Dipartimento di Chimica, Università "La Sapienza", P.le A. Moro 5, Rome I-00185, Italy

ABSTRACT A combination of experimental and theoretical work strongly implicates the production of vinylidene in the photodissociation of the allyl radical, CH_2CHCH_2, an important intermediate in hydrocarbon combustion. The evidence comes from a study of the dissociation of 2-d_1-allyl, which yields distinctly different translational energy distributions and mechanisms for the products HCCH + CH_2D and DCCH + CH_3. In one mechanism, a 1,3 hydrogen shift takes place to give the CH_3CDCH intermediate, which then dissociates to yield CH_3 + DCCH, whereas in the second, one of two branches occurs after a 1,2 hydrogen shift. The shift forms $CH_2D-C-CH_2$, which either dissociates directly to CH_2D + CCH_2 (vinylidene) or undergoes a second 1,2 shift to give $CH_2D-CH-CH$, which subsequently dissociates to CH_2D + HCCH.

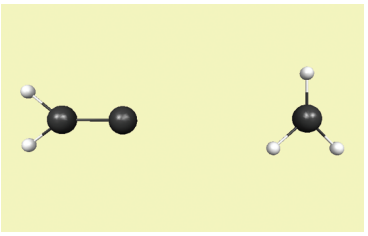

SECTION Kinetics, Spectroscopy

Vinylidene, the high-energy isomer of acetylene, is an important, highly reactive carbene that plays a central role in synthetic organic chemistry.[1] As such, it has attracted the attention of physical chemists who have tried, largely unsuccessfully, to isolate and detect vinylidene spectroscopically. Several experimental reports of the fleeting existence of vinylidene have appeared,[2−4] even as the spectroscopic search for vinylidene continues.[5−8] Guided by the first experiment,[2] early theoretical work assumed a transient existence for vinylidene and estimated a lifetime for it.[9] However, later work based on an accurate full-dimensional potential energy surface and vibrational analysis has demonstrated the existence of molecular eigenstates with clear characteristics of stable vinylidene.[10−12] Therefore, from this work, there is a degree of confidence in its existence and stability. In this Letter, we present strong evidence from recent theory and experiment on the photodissociation of 2-d_1-allyl,[13] implicating vinylidene as a product of this dissociation. In addition, this Letter resolves a puzzle related to the translational energy distributions of the two sets of products observed in these experiments.

As noted, the experiment that motivated the present theoretical work reported different translational energy distributions, denoted $P(E_{trans})$, of the molecular products CH_3 + DCCH and CH_2D + HCCH following photoexcitation of CH_2CDCH_2 (2-d_1-allyl) at 248 nm.[13] It was found that $P(E_{trans})$ for the former peaks at about 15 kcal/mol, and that for the latter was at about 6 kcal/mol. This result was surprising because both pathways would be expected to pass through an intermediate of the form (for the nondeuterated species) $CH_3-CH-CH$. The conventional description of the dissociation, based on the widely used RRKM theory,[14] is that energy will be randomized in the potential energy well of this intermediate before dissociation, so that one would expect the two isotopically different products to have nearly the same kinetic energy distributions, contrary to observation.

Thus, we undertook a full-dimensional dynamical study of this unimolecular reaction by first developing a global potential energy surface (PES) for CH_2CHCH_2, including a description of the H-atom elimination channels. The construction of the PES employs procedures developed previously in our group.[15,16] It is made explicitly invariant under all permutations of like nuclei, and this property is expressed by the polynomial basis used for the fitting.[16] The invariant polynomials, of maximum degree five, are functions of Morse-type variables y_{ij} given by $y_{ij} = \exp(-r_{ij}/\lambda)\}$, where r_{ij} is the internuclear distance between nuclei i and j. The associated 3308 coefficients were obtained by standard linear-least-squares fitting to a data set of 97 418 ab initio energies, computed at the coupled cluster single, double, and perturbative treatment of triple excitations (CCSD(T)) with the augmented correlation-consistent polarized triple basis set (aug-cc-pVTZ) as implemented in MOLPRO.[17] The configurations include regions of the complex C_3H_5, the separated $CH_3+C_2H_2$, and the product channels for each of the C_3H_4 isomers and hydrogen. Additional energies of about 20 000 fragment configurations were obtained by separating the

Received Date: May 15, 2010
Accepted Date: May 24, 2010

DOI: 10.1021/jz100638v | *J. Phys. Chem. Lett.* **2010**, *1*, 1875–1880

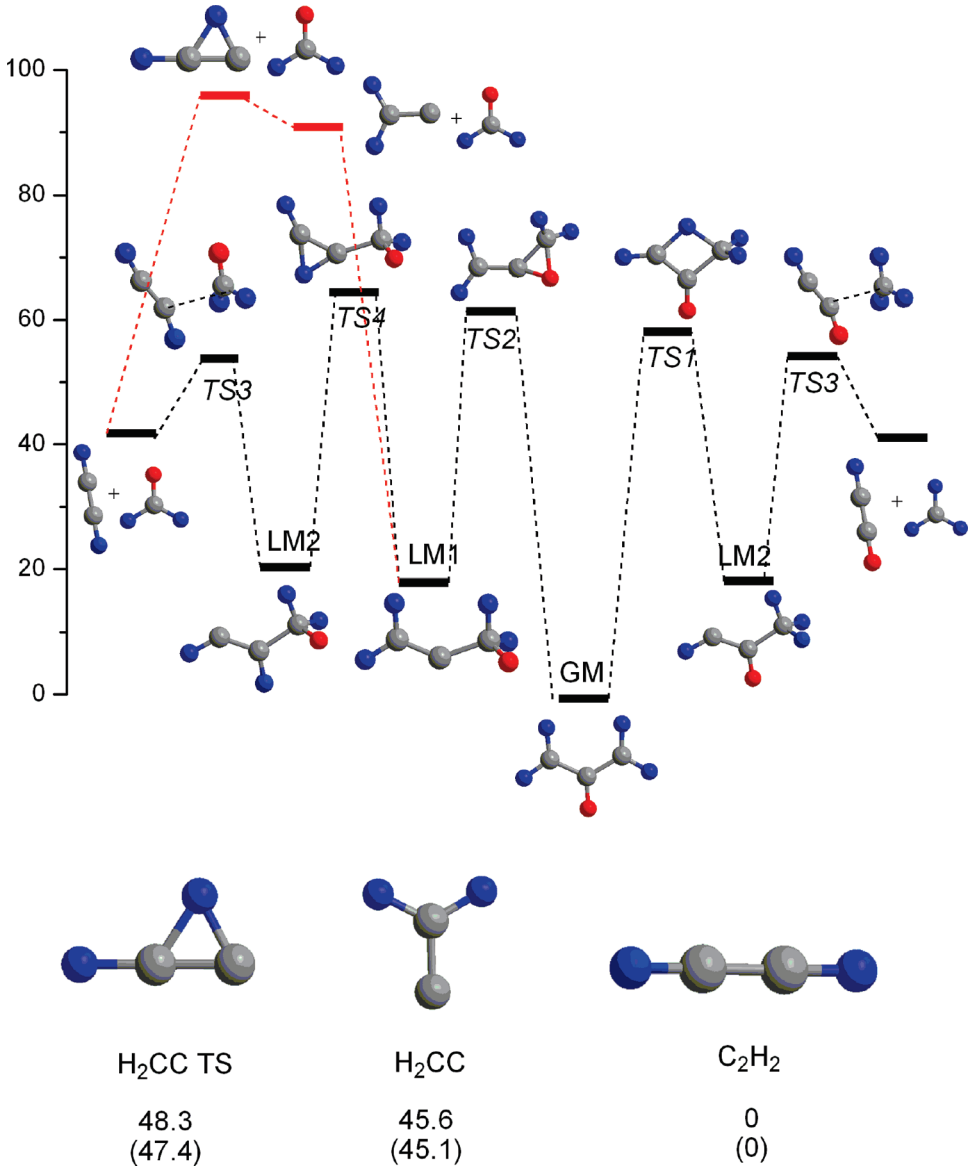

Figure 1. Schematic diagram of the configurations of stationary points of the allyl potential energy surface relevant to the $CH_3 + HCCH$ channel. Energies and harmonic frequencies of these configurations are given in the SI. Also shown above red, solid lines are the geometries and energies of vinylidene, and the barrier for the acetylene/vinylidene isomerization from the PES and from direct ab initio calculations is in parentheses. The energy scale at the left is in kcal/mol relative to GM.

fragments by about 8 bohr, and assigning the energy as the sum of their fragment energies. The rms fitting error is 2.4 kcal/mol for energies up to 63 kcal/mol.

Previous ab initio calculations of various stationary points of the potential have been reported.[13,18,19] These calculations and additional ones that we performed were used to check the fitted PES in Table 1 of the Supporting Information (SI). As seen there, the PES faithfully represents these stationary points and describes the various products well, both in terms of geometry and harmonic frequencies. Of particular relevance to the present study are the stationary points and product channels shown schematically in Figure 1, where the migrating H (or D) atom is colored red. The local minima and transition states are indicated below as LM*n* and TS*m* where *n* and *m* are used in the figure (and as explained in the caption). We can use this notation to indicate the two pathways for the molecular channel noted above as

Pathway (1): single 1,3 shift

$$CH_2CDCH_2(GM) \rightarrow TS1 \rightarrow LM2 \rightarrow TS3 \rightarrow CH_3 + DCCH \quad (1)$$

Pathway (2): double 1,2 shifts

$$CH_2CDCH_2(GM) \rightarrow TS2 \rightarrow LM1 \rightarrow TS4 \rightarrow LM2 \rightarrow TS3 \rightarrow CDH_2 + HCCH \quad (2)$$

The difference between the two pathways is whether or not the dissociation samples the potential energy well

DOI: 10.1021/jz100638v | J. Phys. Chem. Lett. 2010, 1, 1875–1880

around LM1. Those that sample the potential well were counted as contributing to the double 1,2 hydrogen-shift channel in Stranges et al.,[13] whereas those that bypass this potential energy well were counted as contributing to the 1,3 hydrogen-shift channel. These were distinguished by different products when starting with the 2-d_1-allyl radical.[13]

Also, anticipating the results of the trajectory calculations, we indicate in Figure 1 the geometries and energetics of the isomerization of acetylene to vinylidene from the PES and from high-level ab initio calculations.[19] As seen, the PES does describe this isomerization quite accurately, and therefore, the possibility to form vinylidene in this dissociation is at least not precluded in the PES.

Trajectory Calculations. The quasi-classical trajectory calculations were performed using methods similar to those used previously.[20] Calculations were done in a space-fixed frame using microcanonical sampling of initial momenta subject to the zero total angular momentum constraint. Roughly 19 000 trajectories were initiated at the global minimum, with a total energy corresponding to 248 nm excitation plus harmonic zero-point energy. The integration was done using time steps of 0.1205 fs, and trajectories were run for typically 200 000 steps or 24.1 ps (in some cases, 100 000 steps or about 12 ps). For mechanistic analysis, roughly 2750 trajectories were also initiated from LM1, and roughly 500 were initiated from LM2, at this total energy.

Analysis Methods. Trajectories were analyzed by first assigning a structure to the products. A program automatically classified the final configuration into several categories, such as H + allene, H + propyne, H + other C_3H_4 products, and $CH_3 + C_2H_2$. Since the trajectory keeps track of the identities of the different carbons and hydrogens, it is possible to further categorize the results. Thus, for the $CH_3 + C_2H_2$ category, the products were examined to see whether they were consistent with a 1,3 hydrogen shift mechanism (eq 1) or a double 1,2 hydrogen shift mechanism (eq 2). There are multiple variants for each reaction depending on which hydrogen(s) are transferred. Once the final structure has been determined, it is a simple matter to determine the relative velocity of the two fragments in the center-of-mass frame. This velocity was used to determine the kinetic energy distribution.

The methyl elimination channels starting from C_3H_5 and CH_2CDCH_2 are very similar; the $P(E_{trans})$ distributions are nearly identical, except for a slight shift to smaller energies for the deuterated compound, as expected from the slightly larger mass.

Methyl elimination channels were identified by examining the final products to see whether they were consistent with a 1,3 hydrogen shift mechanism (eq 1) or a double 1,2 hydrogen shift (eq 2). The kinetic energy distributions for these two groups can then be determined separately and compared to the data of Stranges et al.[13] The top panel of Figure 2 shows that, indeed, the distribution for the dissociation of C_3H_5 via pathway 1 peaks at a higher kinetic energy (about 14 kcal/mol) than does the distribution for dissociation via pathway 2. The distributions from the trajectory results are in reasonable agreement with the experimental data. As noted before, this is particularly surprising on RRKM grounds since the

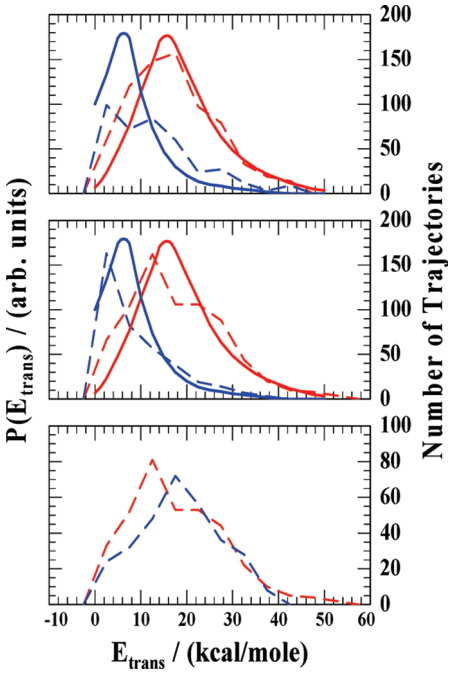

Figure 2. Top Panel: The solid curves give the experimental kinetic energy distributions for HCCH (blue) and DCCH (red) from ref 13. The dashed curves give the corresponding distributions for trajectories starting at the allyl global minimum for C_3H_5 and producing HCCH (blue, ×3) and DCCH (red). Middle Panel: The heavy smooth curves are as in the top panel. The dashed curves are for methyl-producing trajectories starting in LM1 (blue) and LM2 (red). Bottom Panel: Comparison of the translational energy distributions for methyl-producing trajectories starting from LM2 (red) or LM1 (blue, ×4), where the latter trajectories include only those that undergo a second 1,2 shift; that is, vinylidene-producing trajectories are eliminated from the distribution.

presumed pathways 1 and 2 both traverse LM2 before dissociation. The reason for the difference will be made clear below.

In order to investigate the methyl elimination channels in more detail, we ran trajectories starting from LM1 and LM2. For all of the trajectories that produced methyl, we determined the kinetic energy distribution in each case. These are plotted in the middle panel of Figure 2. As can be seen from a comparison of the top and middle panels, the distributions obtained starting in these local minima are similar to those found for trajectories starting at the global minimum. Thus, for diagnostic purposes, it is sufficient to run trajectories from LM1 and LM2.

Trajectories that start from LM1 and proceed via a second 1,2 shift (and isomerize to LM2) produce, as expected, a nearly identical kinetic energy distribution to that for trajectories producing products but starting from LM2. Both distributions have average energies of about 18 kcal/mol. It thus appears that the RRKM assumption is correct; trajectories passing through the LM2 potential energy well do produce nearly identical kinetic energy distributions, regardless of how they get to this potential energy well.

The surprising result, which explains the paradox of why the two kinetic energy distributions are not identical, came from close examination of the trajectories starting from LM1.

DOI: 10.1021/jz100638v | J. Phys. Chem. Lett. 2010, 1, 1875–1880

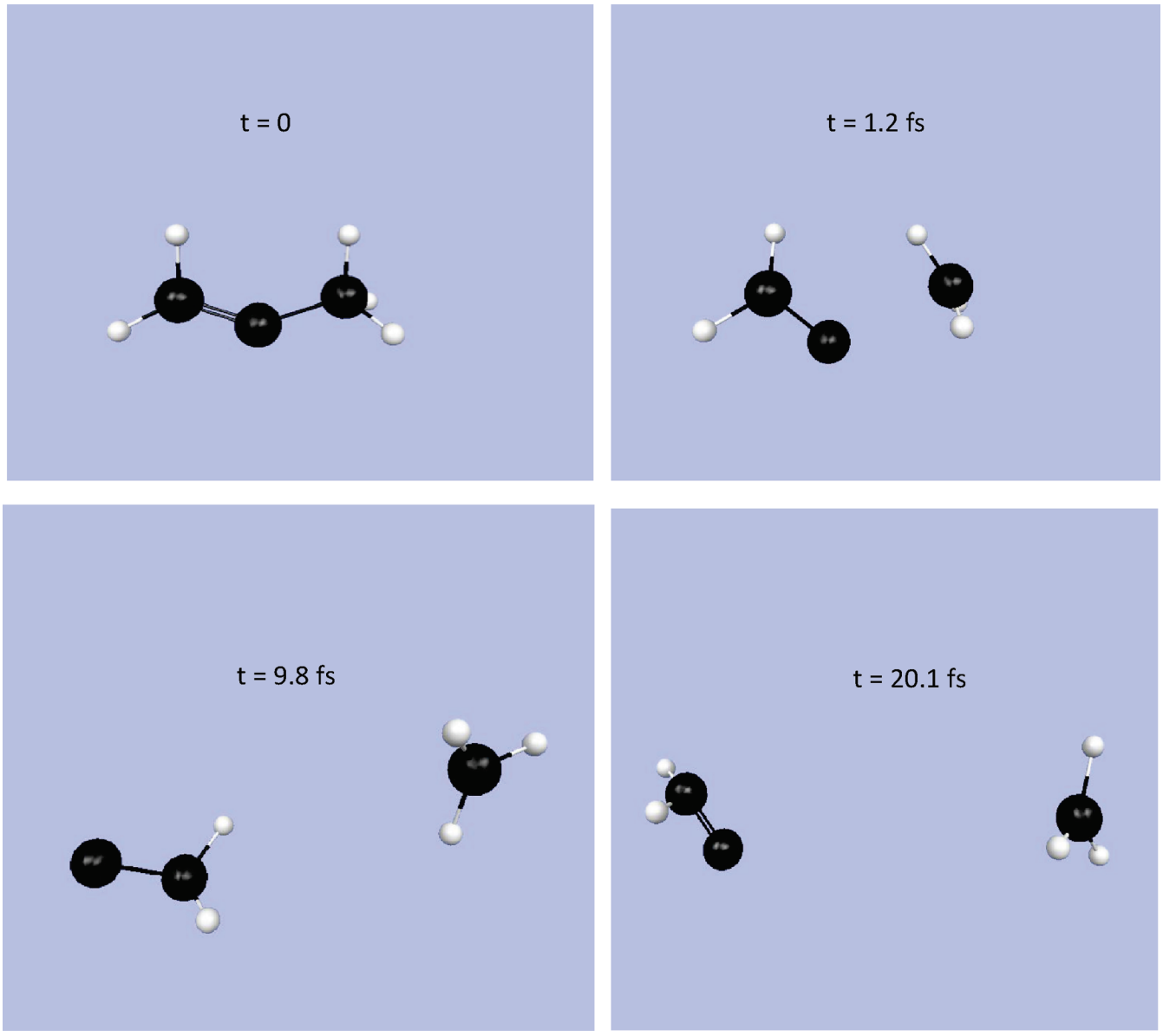

Figure 3. Frames of a classical trajectory initiated from local minimum LM1 leading to formation of vinylidene plus CH_3.

Those producing methyl were of two kinds, the ones that underwent the second 1,2 hydrogen shift and those that dissociated directly to vinylidene, representing a third pathway:

$$CH_3CCH_2 \rightarrow CH_3 + CCH_2 \qquad (3)$$

In more than half of the trajectories starting from LM1 (CH_3CCH_2), the C−C bond broke well before a hydrogen from the CH_2 group migrated to the center carbon. Although the trajectories typically stopped soon after the C−C bond was broken, the CCH_2 clearly had sufficient energy to rearrange to HCCH. On the other hand, the acetylene produced from vinylidene was created with a very large degree of vibrational energy, leaving much less energy available as kinetic energy of recoil. The kinetic energy distribution for the products of a configuration consistent with pathway 2 is therefore peaked at lower energy than that for products of a configuration consistent with pathway 1. Thus, the trajectory results strongly suggest that the distribution attributed to eq 2 actually consists of a mixture of trajectories, those that undergo the second 1,2 shift (eq 2) and those that produce vinylidene (eq 3). Most of those that produce vinylidene do isomerize to highly excited acetylene. The kinetic energy distribution for those C_3H_5 trajectories starting in LM1 that produce vinylidene peaks near zero and has an average kinetic energy of only 6.4 kcal/mol. Those that produce acetylene via the second 1,2 shift have a translational energy distribution nearly identical to that for trajectories producing products but starting from LM2, as shown in the bottom panel of Figure 2.

Figure 3 shows frames of a trajectory, with the times indicated, that starts from LM1 and that forms vinylidene

DOI: 10.1021/jz100638v | J. Phys. Chem. Lett. 2010, 1, 1875–1880

and yields a small relative translational energy of the H_2CC and CH_3 products. This particular trajectory proceeds "promptly" to the products. By contrast, trajectories that start at the global minimum take much longer to form the molecular products. Frames of a trajectory initiated there are shown in the SI.

As noted above, trajectories were also run for (experimentally relevant) CH_2CDCH_2. As expected based on the results for CH_2CHCH_2, both pathways 2 and 3 produce products in which the deuterium ends up in the methyl fragment and the acetylene has two hydrogens. Thus, detection of the kinetic energy distributions by mass spectrometry would associate the detection of C_2H_2 to both reactions 2 and 3 while associating the detection of C_2HD to reaction 1.

It is important to investigate why the vinylidene channel is so important, even though this channel is 26.7 kcal/mol higher than the transition state TS4. As a first step to elucidate this, we ran trajectories starting at LM1 as a function of total energy. We determined the total rate of reaction from LM1 and the quantum yields for dissociation to methyl via the vinylidene channel and the channel requiring a second 1,2 hydrogen shift. (The rate for a specific channel is given by the product of the overall rate and the quantum yield for that channel.) From this analysis, it is clear that the 1,2 shift channel dominates at very low energies, but at the higher energies (relevant to the 248 nm photodissociation), the vinylidene channel dominates. This suggests that entropic effects play a decisive role as the energy increases, and these favor the "loose" transition state of the vinylidene channel over the relatively "tight" transition state TS4. As such, it is possible that standard statistical approaches may be able to describe this unusual dissociation.

From a broader perspective, the allyl dissociation has similarities to a number of dissociations recently characterized by "roaming" mechanisms.[21−29] For example, in both formaldehyde and acetaldehyde, it was found that, in addition to direct dissociation over the lowest-energy barrier to form H_2 + CO or CH_4 + CO, a second channel opens up at somewhat higher energy in which the nearly dissociating fragment, H or CH_3, respectively, returns to abstract a hydrogen from HCO. The same products are formed but by different detailed reaction paths and with different internal energy distributions. In a similar way, the allyl radical here dissociates by two "conventional" channels at low energy (reactions 1 and 2), but a third channel (reaction 3) opens at higher energy, producing the same CH_3 + HCCH products but with a very different internal energy distribution. What the third channel for allyl dissociation has in common with the "roaming" channels in formaldehyde and acetaldehyde is a very loose transition state. As soon as the energy is sufficient to reach this barrier, most of the trajectories dissociate via the path over that barrier, even though it is of higher energy.

In conclusion, the high-energy vinylidene radical is strongly implicated in a pathway for methyl elimination by excited allyl radicals. This previously neglected route to products is the cause of the difference in kinetic energy distributions observed by Stranges et al.[13] Although the threshold for the vinylidene route is higher than those for other channels, it can still play an important role because the transition state is relatively loose. The vinylidene pathway is similar to the roaming channels observed previously for dissociation of formaldehyde[21−24] and acetaldehyde.[25−29] It is also clear from the present study that the role of high-energy isomers of stable molecules should be kept in mind when interpreting high-energy dissociation processes.

SUPPORTING INFORMATION AVAILABLE Full schematic of the potential energy surface of C_3H_5 (including additional minima and transition states describing the H-atom channels), figures and tables comparing the properties of the fitted PES with direct ab initio calculations, a table of principal moments of inertia at stationary points, and frames of a trajectory starting at the global minimum and leading to CH_3 + vinylidene, after first isomerizing to LM1. This material is available free of charge via the Internet at http://pubs.acs.org.

AUTHOR INFORMATION

Corresponding Author:

*To whom correspondence should be addressed. E-mail: joel.bowman@emory.edu (J.M.B.); paul.houston@cos.gatech.edu (P.L.H.).

Present Addresses:

International Atomic Energy Agency, Division of Physical and Chemical Sciences, Vienna, Austria.

ACKNOWLEDGMENT J.M.B. thanks the Department of Energy (DE-FG02-97ER14782) for financial support. Acknowledgment is made to the Donors of The American Chemical Society Petroleum Research Fund for the partial support of this work (No. 46303-AC6) (P.L.H.), and P.L.H. also acknowledges partial support for this work from the National Science Foundation under Award CHE-0852482.

REFERENCES

(1) Stang, P. J. Unsaturated Carbenes. *Chem. Rev.* **1978,** *78*, 383–405.
(2) Ervin, K. M.; Ho, J.; Lineberger, W. C. A Study of the Singlet and Triplet-States of Vinylidene by Photoelectron-Spectroscopy of $H_2C{=}C^-$, $D_2C{=}C^-$, and $HDC{=}C^-$ — Vinylidene Acetylene Isomerization. *J. Chem. Phys.* **1989,** *91*, 5974–5992.
(3) Ervin, K. M.; Gronert, S.; Barlow, S. E.; Gilles, M. K.; Harrison, A. G.; Bierbaum, V. M.; Depuy, C. H.; Lineberger, W. C.; Ellison, G. B. Bond Strengths of Ethylene and Acetylene. *J. Am. Chem. Soc.* **1990,** *112*, 5750–5759.
(4) Jacobson, M. P.; Field, R. W. Acetylene at the Threshold of Isomerization. *J. Phys. Chem. A* **2000,** *104*, 3073–3086.
(5) Levin, J.; Feldman, H.; Baer, A.; Ben-Hamu, D.; Heber, O.; Zajfman, D.; Vager, Z. Study of Unimolecular Reactions by Coulomb Explosion Imaging: The Nondecaying Vinylidene. *Phys. Rev. Lett.* **1998,** *81*, 3347–3350.
(6) Osipov, T.; Cocke, C. L.; Prior, M. H.; Landers, A.; Weber, T.; Jagutzki, O.; Schmidt, L.; Schmidt-Bocking, H.; Dorner, R. Photoelectron−Photoion Momentum Spectroscopy as a Clock for Chemical Rearrangements: Isomerization of the Di-Cation of Acetylene to the Vinylidene Configuration. *Phys. Rev. Lett.* **2003,** *90*, 233002.
(7) Liu, D. K.; Letendre, L. T.; Dai, H. L. 193 nm Photolysis of Vinyl Bromide: Nascent Product Distribution of the $C_2H_3Br \rightarrow C_2H_2$ (Vinylidene) Plus HBr Channel. *J. Chem. Phys.* **2001,** *115*, 1734–1741.
(8) Carvalho, A.; Hancock, G.; Saunders, M. The Reaction Products of the 193 nm Photolysis of Vinyl Bromide and Vinyl

DOI: 10.1021/jz100638v | *J. Phys. Chem. Lett.* **2010,** *1*, 1875–1880

Chloride Studied by Time-Resolved Fourier Transform Infrared Emission Spectroscopy. *Phys. Chem. Chem. Phys.* **2006,** *8*, 4337–4346.
(9) Carrington, T.; Hubbard, L. M.; Schaefer, H. F.; Miller, W. H. Vinylidene — Potential-Energy Surface and Unimolecular Reaction Dynamics. *J. Chem. Phys.* **1984,** *80*, 4347–4354.
(10) Zou, S.-L.; Bowman, J. M.; Brown, A. Full-dimensionality Quantum Calculations of Acetylene−Vinylidene Isomerization. *J. Chem. Phys.* **2003,** *118*, 10012–10023.
(11) Kozin, I. N.; Law, M. M.; Tennyson, J.; Hutson, J. M. Calculating Energy Levels of Isomerizing Tetra-Atomic Molecules. II. The Vibrational States of Acetylene and Vinylidene. *J. Chem. Phys.* **2005,** *122*, 064309.
(12) Tremblay, J. C.; Carrington, T. Calculating Vibrational Energies and Wave Functions of Vinylidene Using a Contracted Basis with a Locally Reorthogonalized Coupled Two-Term Lanczos Eigensolver. *J. Chem. Phys.* **2006,** *125*, 094311.
(13) Stranges, D.; O'Keeffe, P.; Scotti, G.; Di Santo, R.; Houston, P. L. Competing Sigmatropic Shift Rearrangements in Excited Allyl Radicals. *J. Chem. Phys.* **2008,** *128*, 151101.
(14) See, for example, section 7.5.4. in: Houston, P. L. *Chemical Kinetics and Reaction Dynamics*; Dover: New York, 2001.
(15) Chen, C.; Shepler, B. C.; Braams, B. J.; Bowman, J. M. Quasiclassical Trajectory Calculations of the OH + NO_2 Association Reaction on a Global Potential Energy Surface. *J. Chem. Phys.* **2007,** *127*, 104310.
(16) For a recent review, see: Braams, B. J.; Bowman, J. M. Permutationally Invariant Potential Energy Surfaces in High Dimensionality. *Int. Rev. Phys. Chem.* **2009,** *28*, 577–606.
(17) Werner, H. J.; Knowles, P. J.; Lindh, R.; Manby, F. R.; Schutz, M.; Celani, P.; Korona, T.; Rauhut, G.; Amos, R. D.; Bernhardsson, A.; Berning, A.; et al. *MOLPRO*, 2006.1 ed.; **2006**.
(18) Castiglioni, L.; Bach, A.; Chen, P. Spectroscopy and Dynamics of A [B-2(1)] Allyl Radical. *Phys. Chem. Chem. Phys.* **2006,** *8*, 2591–2598.
(19) Chang, N. Y.; Shen, M. Y.; Yu, C. H. Extended *Ab Initio* Studies of the Vinylidene−Acetylene Rearrangement. *J. Chem. Phys.* **1997,** *106*, 3237–3242.
(20) Shepler, B. C.; Braams, B. J.; Bowman, J. M. "Roaming" Dynamics in CH_3CHO Photodissociation Revealed on a Global Potential Energy Surface. *J. Phys. Chem. A* **2008,** *112*, 9344–9351.
(21) Townsend, D.; Lahankar, S. A.; Lee, S. K.; Chambreau, S. D.; Suits, A. G.; Zhang, X.-B.; Rheinecker, J.; Harding, L. B.; Bowman, J. M. The Roaming Atom: Straying from the Reaction Path in Formaldehyde Decomposition. *Science* **2004,** *306*, 1158–1161.
(22) Bowman, J. M.; Zhang, X.-B. New Insights on Reaction Dynamics from Formaldehyde Photodissociaton. *Phys. Chem. Chem. Phys.* **2006,** *8*, 321–332.
(23) Suits, A. G. Roaming Atoms and Radicals: A New Mechanism in Molecular Dissociation. *Acc. Chem. Res.* **2008,** *41*, 873–881.
(24) Goncharov, V.; Lahankar, S. A.; Farnum, J. D.; Bowman, J. M.; Suits, A. G. Roaming Dynamics in Formaldehyde-d_2 Dissociation. *J. Phys. Chem. A* **2009,** *113*, 15315–15319.
(25) Houston, P. L.; Kable, S. H. Photodissociation of Acetaldehyde as a Second Example of the Roaming Mechanism. *Proc. Natl. Acad. Sci. U.S.A.* **2006,** *103*, 16079–16082.
(26) Bowman, J. M. Skirting the Transition State, a New Paradigm in Reaction Rate Theory [Commentary]. *Proc. Natl. Acad. Sci. U.S.A.* **2006,** *103*, 16061–16062.
(27) Rubio-Lago, L.; Amaral, G. A.; Arregui, A.; Izquierdo, J. G.; Wang, F.; Zaouris, D.; Kitsopoulos, T. N.; Banares, L. Slice Imaging of the Photodissociation of Acetaldehyde at 248 nm. Evidence of a Roaming Mechanism. *Phys. Chem. Chem. Phys.* **2007,** *9*, 6123–6127.
(28) Heazlewood, B. R.; Jordan, M. J. T.; Kable, S. H.; Selby, T. M.; Osborn, D. L.; Shepler, B. C.; Braams, B. J.; Bowman, J. M. Roaming is the Dominant Mechanism for Molecular Products in Acetaldehyde Photodissociation. *Proc. Natl. Acad. Sci. U.S.A.* **2008,** *105*, 12719–12724.
(29) Harding, L. B.; Georgievskii, Y.; Klippenstein, S. J. Roaming Radical Kinetics in the Decomposition of Acetaldehyde. *J. Phys. Chem. A* **2010,** *114*, 765–777.

DOI: 10.1021/jz100638v | *J. Phys. Chem. Lett.* **2010,** *1*, 1875–1880